Measurement of the Sensitivity Function in a Time-Domain Atomic Interferometer

Patrick Cheinet, Benjamin Canuel, Franck Pereira Dos Santos, Alexandre Gauguet, Florence Yver-Leduc, and Arnaud Landragin

***Abstract*—We present here an analysis of the sensitivity of a time-domain atomic interferometer to the phase noise of the lasers used to manipulate the atomic wave packets. The sensitivity function is calculated in the case of a three-pulse Mach–Zehnder interferometer, which is the configuration of the two inertial sensors we are building at the Laboratoire National de Métrologie et d'Essais-Système de Références Temps-Espace. We successfully compare this calculation to experimental measurements. The sensitivity of the interferometer is limited by the phase noise of the lasers as well as by residual vibrations. We evaluate the performance that could be obtained with state-of-the-art quartz oscillators, as well as the impact of the residual phase noise of the phase-locked loop. Requirements on the level of vibrations are derived from the same formalism.**

***Index Terms*—Atomic physics, gyroscopes, interferometry, laser noise, phase-locked loops (PLLs), phase noise, vibrations.**

I. Introduction

ATOM optics are a means to realize precision measurements in various fields. Atomic microwave clocks are the most precise realization of a Système Internationale unit, namely, the second [1], and high-sensitivity inertial sensors [2]–[4], based on atomic interferometry [5], already reveal accuracies that are comparable with state-of-the-art sensors [6], [7]. Two cold atom inertial sensors are currently under construction at the Laboratoire National de Métrologie et d'Essais-Système de Références Temps-Espace (LNE-SYRTE)—a gyroscope [8], which already reaches a sensitivity of 2.5×10^{-6} rad $\cdot$ s^{-1} $\cdot$ Hz$^{-1/2}$, and an absolute gravimeter [9], which will be used in the LNE watt Balance project [10]. Although based on different atoms and geometries, the atomic gyroscope and gravimeter rely on the same principle, which is presented in Fig. 1. Atoms are collected in a 3-D magnetooptical trap (3-D-MOT) in which the atoms are cooled down to a few microkelvins. In the gyroscope, ^{133}Cs atoms are launched upward with an angle of 8°, with respect to verticality using the technique of moving molasses, whereas in the gravimeter, ^{87}Rb atoms are simply allowed to fall. Then, the initial quantum state is prepared by a combination of microwave and optical pulses. The manipulation of the atoms is realized by stimulated Raman transition pulses [11], using two counterpropagating lasers, which drive coherent transitions between the two hyperfine levels of the alkali atom. Three laser pulses, of durations τ_R, $2\tau_R$, and τ_R, separated in time by T, respectively split, redirect, and recombine the atomic wave packets, creating an atomic interferometer [12]. Finally, a fluorescence detection gives a measurement of the transition probability from one hyperfine level to the other, which is given by $P = (1/2)(1 - \cos(\Phi))$, Φ being the interferometric phase. The phase difference between the two Raman lasers (which we will call the Raman phase throughout this paper, and will be denoted as ϕ) is imprinted at each pulse on the phase of the atomic wave function [13]. As ϕ depends on the position of the atoms, the interferometer is sensitive to inertial forces and can thus measure rotation rates and accelerations. A drawback of this technique is that the measurement of the interferometric phase is affected by the phase noise of the Raman lasers as well as parasitic vibrations. The aim of this paper is to investigate both theoretically and experimentally how these noise sources limit the sensitivity of such an atomic interferometer.

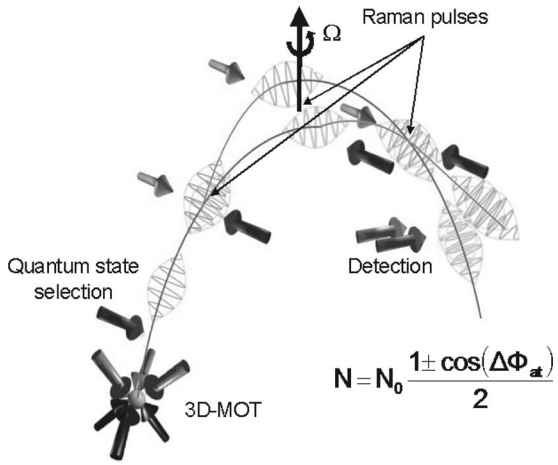

Fig. 1. Scheme of principle of our inertial sensors, which is illustrated for the gyroscope experiment. Cold atoms from the 3-D-MOT are launched upward, and a pure quantum state is selected. At the top of their trajectory, we apply three Raman laser pulses realizing the interferometer. Finally, a fluorescence detection allows measurement of the transition probability. Such an interferometer is sensitive to the rotation (Ω) perpendicular to the area enclosed between the two arms and to the acceleration along the laser's axis.

Manuscript received March 23, 2005; revised November 26, 2007. This work was supported in part by the Laboratoire National de Métrologie et d'Essais (LNE), by the Centre National de la Recherche Scientifique (CNRS), by the Délégation générale pour l'armement (DGA), and by the Centre National d'Études Spatiales (CNES).

P. Cheinet is with the University of Mainz, 55099 Mainz, Germany.

B. Canuel is with the European Gravitational Observatory, 56021 Pisa, Italy.

F. Pereira Dos Santos, A. Gauguet, F. Yver-Leduc, and A. Landragin are with the LNE-Système de Références Temps-Espace (SYRTE), CNRS UMR 8630, Observatoire de Paris, 75014 Paris, France (e-mail: franck.pereira@obspm.fr).

Color versions of one or more of the figures in this paper are available online at http://ieeexplore.ieee.org.

Digital Object Identifier 10.1109/TIM.2007.915148

II. Sensitivity Function

The sensitivity function is a natural tool to characterize the influence of the fluctuations in the Raman phase ϕ on the transition probability [14] and, thus, on the interferometric phase. Let us assume that a phase jump $\delta\phi$ occurs on the Raman phase ϕ at time t during the interferometer sequence, inducing a change of $\delta P(\delta\phi, t)$ in the transition probability. The sensitivity function is then defined by

$$g(t) = 2 \lim_{\delta\phi \to 0} \frac{\delta P(\delta\phi, t)}{\delta\phi}. \tag{1}$$

The sensitivity function can easily be calculated for infinitesimally short Raman pulses. In this case, the interferometric phase Φ can be deduced from the Raman phases ϕ_1, ϕ_2, and ϕ_3 during the three laser interactions, taken at the position of the center of the atomic wave packet, i.e., $\Phi = \phi_1 - 2\phi_2 + \phi_3$ [15]. Usually, the interferometer is operated at $\Phi = \pi/2$, for which the transition probability is one half, to get the highest sensitivity to interferometric phase fluctuations. If the phase step $\delta\phi$ occurs, for instance, between the first and the second pulses, the interferometric phase changes by $\delta\Phi = -\delta\phi$, and the transition probability by $\delta P = -\cos(\pi/2 + \delta\Phi)/2 \sim -\delta\phi/2$ in the limit of an infinitesimal phase step. Thus, in between the first two pulses, the sensitivity function is -1: the same way one finds for the sensitivity function between the last two pulses, i.e., $+1$.

In the general case of finite-duration Raman laser pulses, the sensitivity function depends on the evolution of the atomic state during the pulses. To calculate $g(t)$, we make several assumptions. First, the laser waves are considered as pure plane waves. The atomic motion is then quantized in the direction parallel to the laser beams. Second, we restrict our calculation to the case of a constant Rabi frequency (square pulses). Third, we assume that the resonance condition is fulfilled. The Raman interaction then couples the two states $|a\rangle = |g_1, \overrightarrow{p}\rangle$ and $|b\rangle = |g_2, \overrightarrow{p} + \hbar\overrightarrow{k}_{\text{eff}}\rangle$, where $|g_1\rangle$ and $|g_2\rangle$ are the two hyperfine levels of the ground state, $\overrightarrow{p}$ is the atomic momentum, and $\overrightarrow{k}_{\text{eff}}$ is the difference between the wave vectors of the two lasers.

We develop the atomic wave function on the basis set $\{|a\rangle, |b\rangle\}$ so that $|\Psi(t)\rangle = C_a(t)|a\rangle + C_b(t)|b\rangle$ and choose the initial state to be $|\Psi(t_i)\rangle = |\Psi_i\rangle = |a\rangle$. At the output of the interferometer, the transition probability is given by $P = |C_b(t_f)|^2$, where $t_f = t_i + 2T + 4\tau_R$. The evolution of C_a and C_b from t_i to t_f is given by

$$\begin{pmatrix} C_a(t_f) \\ C_b(t_f) \end{pmatrix} = M \begin{pmatrix} C_a(t_i) \\ C_b(t_i) \end{pmatrix} \tag{2}$$

where M is the evolution matrix through the whole interferometer. Solving the Schrödinger equation gives the evolution matrix (3), shown at the bottom of the page, during a Raman pulse [16], from time t_0 to time t, where $\Omega_R/2\pi$ is the Rabi frequency, and ω_L, which is the effective frequency, is the frequency difference between the two lasers $\omega_L = \omega_2 - \omega_1$. Setting $\Omega_R = 0$ in $M_p(t_0, t, \Omega_R, \phi)$ gives the free evolution matrix, which determines the evolution between the pulses. The evolution matrix for the full evolution is obtained by taking the product of several matrices. When t occurs during the ith laser pulse, we split the evolution matrix of this pulse at time t into two successive matrices—the first one with ϕ_i and the second one with $\phi = \phi_i + \delta\phi$.

Finally, we choose the time origin at the middle of the second Raman pulse. We thus have $t_i = -(T + 2\tau_R)$ and $t_f = T + 2\tau_R$. We then calculate the change in the transition probability for an infinitesimally small phase jump at any time t during the interferometer and deduce $g(t)$. It is an odd function, whose expression is given here for $t > 0$. Thus, we have

$$g(t) = \begin{cases} \sin(\Omega_R t), & 0 < t < \tau_R \\ 1, & \tau_R < t < T + \tau_R \\ -\sin\left(\Omega_R(T - t)\right), & T + \tau_R < t < T + 2\tau_R. \end{cases} \tag{4}$$

When the phase jump occurs outside the interferometer, the change in the transition probability is null, so that $g(t) = 0$ for $|t| > T + 2\tau_R$.

To validate this calculation, we use the gyroscope experiment to experimentally measure the sensitivity function. About 10^8 atoms from a background vapor are loaded in a 3-D-MOT within 125 ms, with six laser beams tuned to the red of the $F = 4 \rightarrow F' = 5$ transition at 852 nm. The atoms are then launched upward at $\sim$2.4 m/s within 1 ms and cooled down to an effective temperature of ~ 2.4 μK. After launch, the atoms are prepared into the $|F = 3, m_F = 0\rangle$ state using a combination of microwave and laser pulses. They first enter a selection cavity tuned to the $|F = 4, m_F = 0\rangle \rightarrow |F = 3, m_F = 0\rangle$ transition. The atoms left in the $F = 4$ state are pushed away by a laser beam tuned to the $F = 4 \rightarrow F' = 5$ transition, 11 cm above the selection cavity. The selected atoms then reach the apogee 245 ms after the launch, where they experience three interferometer pulses of duration $\tau_R - 2\tau_R - \tau_R$ with $\tau_R = 20$ μs separated in time by $T = 4.97$ ms. The number of atoms $N_{F=3}$ and $N_{F=4}$ are finally measured by detecting the fluorescence induced by a pair of laser beams located 7 cm below the apogee. From these measurements, we deduce the transition probability $N_{F=4}/(N_{F=3} + N_{F=4})$. The total number of detected atoms is about 10^5. The repetition rate of the experiment is 2 Hz.

The setup for the generation of the two Raman laser beams is displayed in Fig. 2. Two slave diode lasers of 150-mW output power are injected with extended cavity diode lasers. The polarizations of the slave diode output beams are made orthogonal so that the two beams can be combined onto a polarization beam splitter cube. The light at this cube is then split in two distinct unbalanced paths.

$$M_p(t_0, t, \Omega_R, \phi) = \begin{pmatrix} e^{-i\omega_a(t-t_0)} \cos\left(\frac{\Omega_R}{2}(t - t_0)\right) & -ie^{-i\omega_a(t-t_0)} e^{i(\omega_L t_0 + \phi)} \sin\left(\frac{\Omega_R}{2}(t - t_0)\right) \\ -ie^{-i\omega_b(t-t_0)} e^{-i(\omega_L t_0 + \phi)} \sin\left(\frac{\Omega_R}{2}(t - t_0)\right) & e^{-i\omega_b(t-t_0)} \cos\left(\frac{\Omega_R}{2}(t - t_0)\right) \end{pmatrix} \tag{3}$$

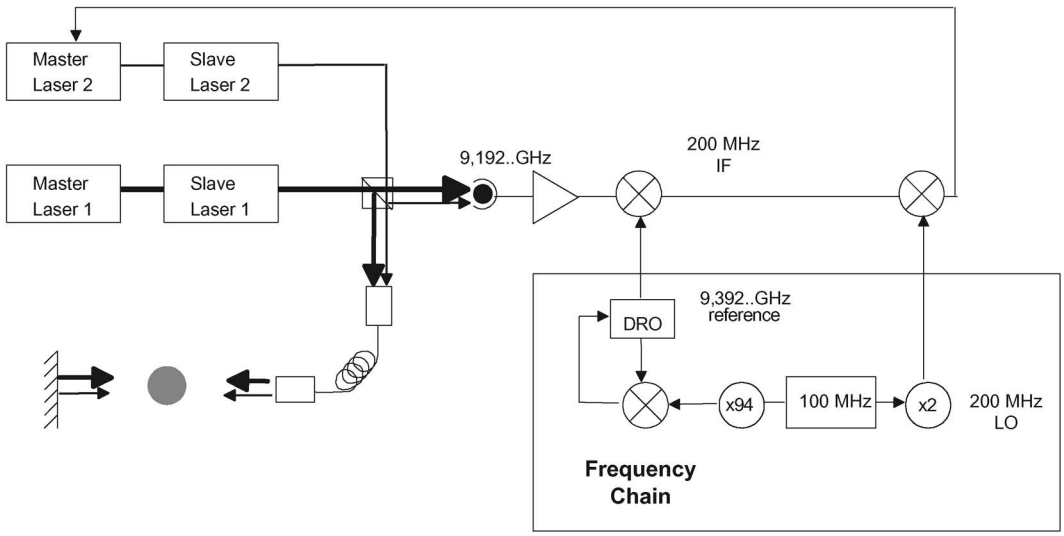

Fig. 2. Principle of the laser phase lock. The beatnote at 9.192 GHz between the two Raman lasers is observed on a fast response photodetector. After amplification, this beatnote is mixed with the reference frequency at 9.392 GHz from the frequency chain to obtain a signal at 200 MHz. This signal is compared with the reference frequency at 200 MHz from the same frequency chain to get an error signal. This error signal is then processed and sent to the current of the laser and to the PZT that controls the laser cavity length.

On the first path, most of the power of each beam is sent through an optical fiber to the vacuum chamber. The two beams are then collimated with an objective attached onto the chamber (waist $w_0 = 15$ mm). They enter together through a viewpoint, cross the atomic cloud, and are finally retroreflected by a mirror fixed outside the vacuum chamber. In this geometry, four laser beams are actually sent onto the atoms, which interact with only two of them, because of selection rules and resonance conditions. The interferometer can also be operated with co-propagating Raman laser beams by simply blocking the light in front of the retroreflecting mirror. A remarkable feature of this experiment is that the three interferometer pulses are realized by this single pair of Raman lasers that is turned on and off three times, the middle pulse being at the top of the atoms' trajectory. For all the measurements described in this paper, the Raman lasers are used in the *copropagating* configuration. The interferometer is then no longer sensitive to inertial forces but remains sensitive to the relative phase of the Raman lasers. Moreover, as such Raman transitions are not velocity selective, more atoms contribute to the signal. All this allows us to reach a good signal to noise ratio of 150 per shot. We insist here on the fact that the formalism developed in this paper does not depend on the geometry of the Raman beams. We test the model with copropagating Raman measurements, but it applies as well to the case of counterpropagating measurements.

The second path is used to control the Raman laser phase difference, which needs to be locked [17] onto the phase of a very stable microwave oscillator. The phase-locked loop (PLL) scheme is also displayed in Fig. 2. The frequency difference is measured by a fast photodetector, which detects a beatnote at 9.192 GHz. This signal is then mixed with the signal of a dielectric resonator oscillator (DRO) tuned at 9.392 GHz. The DRO itself is phase locked onto the 94th harmonics of a very stable 100-MHz quartz. The output of the mixer (IF) is 200 MHz. A local oscillator (LO) at 200 MHz is generated by doubling the same 100-MHz quartz. IF and LO are compared

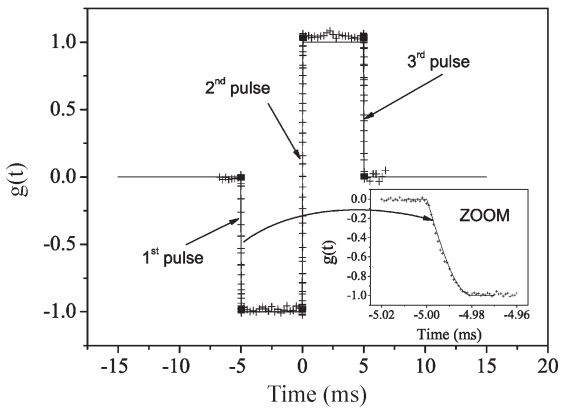

Fig. 3. Atomic sensitivity function $g(t)$ as a function of time for a three-pulse interferometer with a Rabi frequency $\Omega_R = (\pi/2\tau_R)$. The theoretical calculation is displayed in solid line and the experimental measurement in crosses. A zoom is made on the first pulse.

using a digital phase and frequency detector, whose output is used as the error signal of the PLL. The relative phase of the lasers is stabilized by reacting on the current of one of the two diode lasers, as well as on the voltage applied to the piezoelectric transducer (PZT) that controls the length of the extended cavity diode laser [17].

To measure $g(t)$, a small phase step of $\delta\phi = 0.107$ rad is applied at time t on the LO. The PLL copies this phase step onto the Raman phase within a fraction of a microsecond, which is much shorter than the Raman pulse duration of $\tau_R = 20$ μs. Finally, we measured the transition probability as a function of t and deduced the sensitivity function. We display in Fig. 3 the measurement of the sensitivity function compared with the theoretical calculation. We also realized a precise measurement during each pulse and clearly obtained the predicted sinusoidal rise of the sensitivity function.

For a better agreement of the experimental data with the theoretical calculation, the data are normalized to take into

account the interferometer's contrast, which was measured to be 78%. This reduction in the contrast with respect to 100% is due to the combined effect of inhomogeneous Rabi frequencies between the atoms and unbalanced Rabi frequencies between the pulses. Indeed, the atomic cloud size of 8 mm is not negligible with respect to the size of the single pair of Raman Gaussian beams: $w_0 = 15$ mm. Atoms at both sides of the atomic cloud will not see the same intensity, inducing variable transfer efficiency of the Raman transitions. Moreover, the cloud moves by about 3 mm between the first and the last pulse. In order for the cloud to explore only the central part of the Gaussian beams, we choose a rather small interaction time of $T = 4.97$ ms with respect to the maximum interaction time possible of $T = 40$ ms. Still, the quantitative agreement is not perfect. One particularly observes a significant asymmetry of the sensitivity function, which remains to be explained. A full numerical simulation could help in understanding the effect of the experimental imperfections.

III. Transfer Function of the Interferometer

From the sensitivity function, we can now evaluate the fluctuations of the interferometric phase Φ for an arbitrary Raman phase noise $\phi(t)$ on the lasers as

$$\delta\Phi = \int_{-\infty}^{+\infty} g(t)d\phi(t) = \int_{-\infty}^{+\infty} g(t)\frac{d\phi(t)}{dt}dt. \tag{5}$$

The transfer function of the interferometer can be obtained by calculating the response of the interferometer phase Φ to a sinusoidal modulation of the Raman phase, given by $\phi(t) = A_0\cos(\omega_0 t + \psi)$. We find $\delta\Phi = A_0\omega_0 Im(G(\omega_0))\cos(\psi)$, where G is the Fourier transform of the sensitivity function. Thus, we have

$$G(\omega) = \int_{-\infty}^{+\infty} e^{-i\omega t}g(t)dt. \tag{6}$$

When averaging over a random distribution of the modulation phase ψ, the rms value of the interferometer phase is $\delta\Phi^{\mathrm{rms}} = |A_0\omega_0 G(\omega_0)|$. The transfer function is thus given by $H(\omega) = \omega G(\omega)$. If we now assume uncorrelated Raman phase noise between successive measurements, the rms standard deviation of the interferometric phase noise $\sigma_\Phi^{\mathrm{rms}}$ is given by

$$(\sigma_\Phi^{\mathrm{rms}})^2 = \int_0^{+\infty} |H(\omega)|^2 S_\phi(\omega)d\omega \tag{7}$$

where $S_\phi(\omega)$ is the power spectral density of the Raman phase.

We calculate the Fourier transform of the sensitivity function and find

$$G(\omega) = \frac{4i\Omega_R}{\omega^2 - \Omega_R^2}\sin\left(\frac{\omega(T+2\tau_R)}{2}\right) \times\left(\cos\left(\frac{\omega(T+2\tau_R)}{2}\right) + \frac{\Omega_R}{\omega}\sin\left(\frac{\omega T}{2}\right)\right). \tag{8}$$

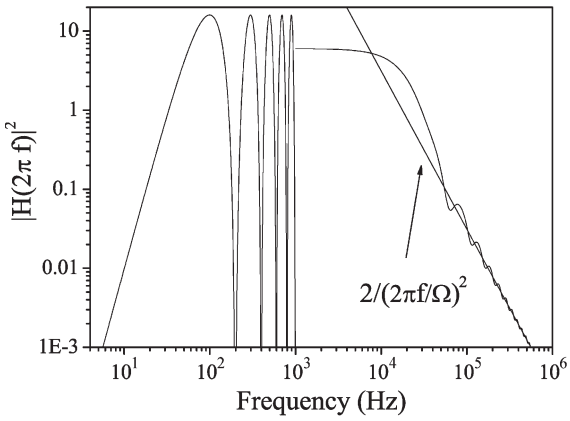

Fig. 4. Calculated weighting function for the Raman phase noise as a function of frequency. Below 1 kHz, the exact weighting function is displayed. It shows an oscillation with a period frequency of $\delta f = 1/(T + 2\tau)$. Above 1 kHz, only the mean value of the weighting function over δf is displayed. The weighting function acts as a first-order low-pass filter, with an effective cutoff frequency of $f_0 = (\sqrt{3}/3)(\Omega_R/2\pi)$.

At low frequency, where $\omega \ll \Omega_R$, the sensitivity function can be approximated by

$$G(\omega) = -\frac{4i}{\omega}\sin^2(\omega T/2). \tag{9}$$

The weighting function $|H(2\pi f)|^2$ versus the frequency f is displayed in Fig. 4. It has two important features. The first one is an oscillating behavior at a frequency given by $1/(T + 2\tau_R)$, leading to zeros at frequencies given by $f_k = k/(T + 2\tau_R)$. The second is a low-pass first-order filtering due to the finite duration of the Raman pulses, with an effective cutoff frequency f_0, given by $f_0 = (\sqrt{3}/3)(\Omega_R/2\pi)$. Above 1 kHz, only the mean value over one oscillation is displayed on the figure.

To measure the transfer function, a phase modulation $A_m\cos(2\pi f_m t + \psi)$ is applied on the Raman phase, triggered on the first Raman pulse. The interferometric phase variation is then recorded as a function of f_m. We then repeat the measurements for the phase modulation in quadrature $A_m\sin(2\pi f_m t + \psi)$. From the quadratic sum of these measurement, we extract $H(2\pi f_m)^2$. The weighting function was first measured at low frequency. The results, which are displayed in Fig. 5 together with the theoretical value, clearly demonstrate the oscillating behavior of the weighting function. Fig. 6 displays the measurements performed slightly above the cutoff frequency and shows two zeros. The first one corresponds to a frequency multiple of $1/(T + 2\tau)$. The second one is a zero of the last factor of (8). Its position depends critically on the value of the Rabi frequency.

When comparing the data with the calculation, the experimental imperfections already mentioned have to be accounted for. An effective Rabi frequency Ω_{eff} can be defined by the relation $\Omega_{\mathrm{eff}}\tau_0 = \pi$, where τ_0 is the duration of the single pulse, performed at the center of the Gaussian Raman beams, that optimizes the transition probability. For homogeneous Raman beams, this pulse would be a π pulse. This effective Rabi frequency is measured with an uncertainty of about 1%. It had to be corrected by only 1.5% in order for the theoretical and experimental positions of the second zero to match. The

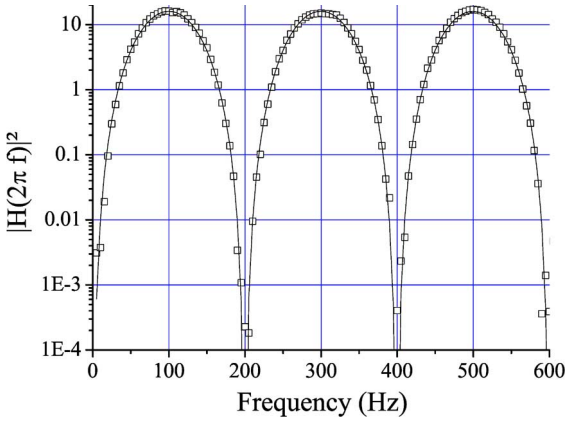

Fig. 5. Phase noise weighting function $|H(2\pi f)^2|$ for $T = 4.97$ ms and $\tau_R = 20$ μs at low frequency. The theoretical calculation is displayed in solid line and the experimental results in squares. We clearly see that the oscillating behavior of the weighting function and the experimental measurement are in good agreement with the theoretical calculation.

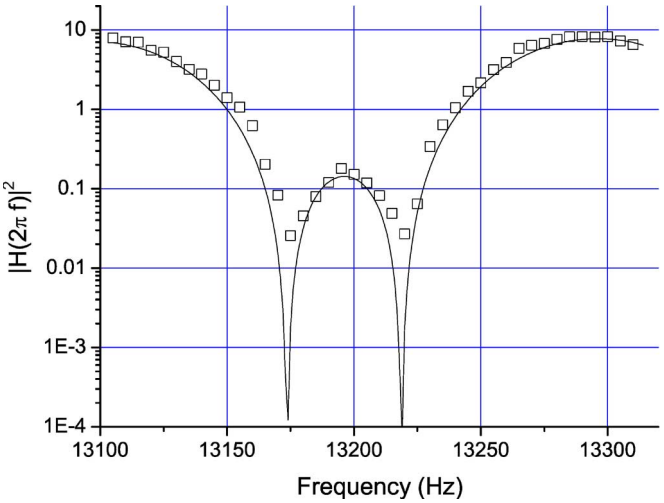

Fig. 6. Phase noise weighting function $|H(2\pi f)^2|$ for $T = 4.97$ ms and $\tau_R = 20$ μs displayed near the Rabi frequency. The theoretical calculation is displayed in solid line and the experimental results in squares. We identified the zero multiple of $(1/T + 2\tau)$ and experimentally observed both zeros with a good agreement with theory.

excellent agreement between the theoretical and experimental curves validates our model.

IV. Link Between the Sensitivity Function and the Sensitivity of the Interferometer

The sensitivity of the interferometer is characterized by the Allan variance of the interferometric phase fluctuations $\sigma_\Phi^2(\tau)$, which is defined as

$$\sigma_\Phi^2(\tau) = \frac{1}{2}\left\langle (\delta\bar{\Phi}_{k+1} - \delta\bar{\Phi}_k)^2 \right\rangle \tag{10}$$

$$= \frac{1}{2}\lim_{n\to\infty}\left\{ \frac{1}{n}\sum_{k=1}^{n} (\delta\bar{\Phi}_{k+1} - \delta\bar{\Phi}_k)^2 \right\} \tag{11}$$

where $\delta\bar{\Phi}_k$ is the average value of $\delta\Phi$ over the interval $[t_k, t_{k+1}]$ of duration τ. The Allan variance is equal, within a factor of two, to the variance of the differences in the successive average values $\delta\bar{\Phi}_k$ of the interferometric phase. Because the interferometer is sequentially operated at a rate $f_c = 1/T_c$, τ is a multiple of T_c : $\tau = mT_c$. Without losing generality, we can choose $t_k = -T_c/2 + kmT_c$. The average value $\delta\bar{\Phi}_k$ can now be expressed as

$$\begin{aligned}\delta\bar{\Phi}_k &= \frac{1}{m}\sum_{i=1}^{m}\delta\Phi_i \\ &= \frac{1}{m}\sum_{i=1}^{m}\int_{t_k+(i-1)T_c}^{t_k+iT_c} g\left(t - t_k - (i-1)T_c - T_c/2\right)\frac{d\phi}{dt}dt \\ &= \frac{1}{m}\int_{t_k}^{t_{k+1}} g_k(t)\frac{d\phi}{dt}dt \end{aligned} \tag{12}$$

where $g_k(t) = \sum_{i=1}^{m} g(t - kmT_c - (i-1)T_c)$. The difference between successive average values is then given by

$$\delta\bar{\Phi}_{k+1} - \delta\bar{\Phi}_k = \frac{1}{m}\int_{-\infty}^{+\infty}\left(g_{k+1}(t) - g_k(t)\right)\frac{d\phi}{dt}dt. \tag{13}$$

For long-enough averaging times, the fluctuations of the successive averages are not correlated, and the Allan variance is given by

$$\sigma_\Phi^2(\tau) = \frac{1}{2}\frac{1}{m^2}\int_0^{+\infty}|G_m(\omega)|^2\,\omega^2 S_\phi(\omega)d\omega \tag{14}$$

where G_m is the Fourier transform of the function $g_{k+1}(t) - g_k(t)$. After a little algebra, we find, for the squared modulus of G_m, the following expression:

$$|G_m(\omega)|^2 = 4\frac{\sin^4(\omega mT_c/2)}{\sin^2(\omega T_c/2)}|G(\omega)|^2. \tag{15}$$

When $\tau\to\infty$, $|G_m(\omega)|^2 \sim (2m/T_c)\sum_{j=-\infty}^{\infty}\delta(\omega - j2\pi f_c)$ $|G(\omega)|^2$. Thus, for large averaging times τ, the Allan variance of the interferometric phase is given by

$$\sigma_\Phi^2(\tau) = \frac{1}{\tau}\sum_{n=1}^{\infty}|H(2\pi n f_c)|^2\,S_\phi(2\pi n f_c). \tag{16}$$

Equation (16) shows that the sensitivity of the interferometer is limited by an aliasing phenomenon similar to the Dick effect in atomic clocks [14]. Only the phase noise at multiple of the cycling frequency appears in the Allan variance, and it is weighted by the Fourier components of the transfer function.

Various sources of phase noise will contribute to (16). Phase noise of the reference oscillator, electronic noise of the PLL, laser phase noise outside the PLL bandwidth, and difference of phase accumulated in the propagation of the two Raman beams to the vacuum chamber will contribute in the same way, whatever the configuration of the Raman beams (copropagating or counterpropagating) is.

In the case of inertial forces, the sensitivity arises from the Raman phase fluctuations of counterpropagating beams in

the referential frame of the atoms and can be treated with the same formalism. As the two laser beams are first overlapped before being sent onto the atoms, their phase difference is mostly affected by the movements of a single optical element, i.e., the mirror that finally retroreflects them. A displacement of the retroreflecting mirror by δz induces a Raman phase shift of $k_{\text{eff}}\delta z$.

V. Laser Phase Noise

In this section, we focus on the influence of the phase noise of the reference oscillator and on the limitations imposed by the PLL.

Let us examine first the case of white Raman phase noise $S_\phi(\omega) = S_\phi^0$. The interferometer sensitivity is given by

$$\sigma_\Phi^2(\tau) = \left(\frac{\pi}{2}\right)^2 \frac{S_\phi^0}{\tau}\frac{T_c}{\tau_R}. \tag{17}$$

In that case, the sensitivity of the interferometer depends not only on the Raman phase noise spectral density but also on the pulse duration τ_R. For a better sensitivity, one should use the largest pulse duration as possible. However, as the Raman transitions are velocity selective in the counterpropagating configuration, a very long pulse will reduce the number of useful atoms. This increases the detection noise contribution, so that there is an optimum value of τ_R that depends on the experimental parameters. In the case of the gyroscope, the optimum was found to be $\tau_R = 20\ \mu$s.

To reach a good sensitivity, the Raman phase needs to be locked to the phase of a very stable microwave oscillator (whose frequency is 6.834 GHz for ^{87}Rb and 9.192 GHz for ^{133}Cs). This oscillator can be generated by a frequency chain, where low phase noise quartz performances are transposed in the microwave domain. At low frequencies ($f < 10{-}100$ Hz), the phase noise spectral density of such an oscillator is usually well approximated by a $1/f^3$ power law (flicker noise), whereas at high frequency ($f > 1$ kHz), it is independent of the frequency (white noise). Using (16) and the typical parameters of our experiments ($\tau_R = 20\ \mu$s and $T = 50$ ms), we can calculate the phase noise spectral density required to achieve an interferometric phase fluctuation of 1 mrad/shot. This is equivalent to the quantum projection noise limit for 10^6 detected atoms. The flicker noise of the microwave oscillator should be lower than -53 dB $\cdot$ rad$^2 \cdot$ Hz^{-1} at 1 Hz from the carrier frequency and its white noise below -111 dB $\cdot$ rad$^2 \cdot$ Hz^{-1}. Unfortunately, there exists no quartz oscillator combining these two levels of performance. Thus, we plan to lock a SC Premium 100 MHz oscillator (from Wenzel Company) onto a low flicker noise 5 MHz Blue Top oscillator (Wenzel). From the specifications of this quartz, we calculate a contribution of 1.2 mrad to the interferometric phase noise.

Phase fluctuations also arise from residual noise in the servo-lock loop. We have experimentally measured the residual phase noise power spectral density of a phase-locked system analogous to the one described in Fig. 2. This system has been developed to phase lock the Raman lasers of the gravimeter experiment. The measurement was performed by mixing IF and LO onto an independent RF mixer, whose output phase fluctuations were analyzed onto a fast Fourier transform analyzer. The result of the measurement is displayed in Fig. 7. At low frequencies, below 100 Hz, the phase noise of our phase-locked system lies well below the required flicker noise. After a few kilohertz, it reaches a plateau of -119 dB $\cdot$ rad$^2 \cdot$ Hz^{-1}. The amplitude of this residual noise is not limited by the gain of the servo loop. Above 60 kHz, it increases up to -90 dB $\cdot$ rad$^2 \cdot$ Hz^{-1} at 3.5 MHz, which is the bandwidth of our servo-lock loop. Using (16), we evaluated to 0.72 mrad its contribution to the interferometer's phase noise.

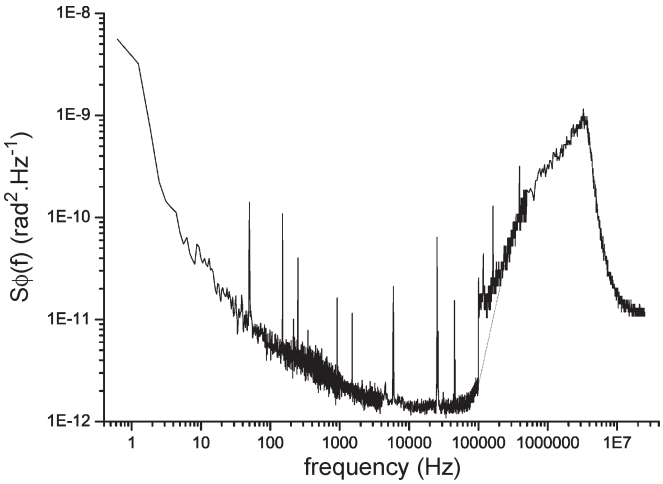

Fig. 7. Phase noise power spectral density between the two phase-locked diode lasers. Up to 100 kHz, we display the residual noise of the PLL, which is obtained by measuring the phase noise of the demodulated beatnote on a fast Fourier transform analyzer. There, the phase noise of the reference oscillator is rejected. Above 100 kHz, we display the phase noise measured directly on the beatnote observed onto a spectrum analyzer. In this case, the reference oscillator phase noise limits the Raman phase noise to 1.5×10^{-11} rad$^2 \cdot$ Hz^{-1}. An extrapolation of the phase noise due to the PLL alone between 100 and 300 kHz is displayed with dotted line.

Other sources of noise are expected to contribute, which are not investigated in this paper. The measurement presented here has been performed with a single optical beat setup, which rejects noise of the photoconductor as well as other noise sources inherent to the setup (vibrations of the mirrors and beamsplitters in the beat setup for instance). Independent measurements we have performed with two independent photoconductors show that these noise sources are anyway negligible—their contribution was found to be on the order of 0.1 mrad/shot. In addition, the phase noise due to the propagation of the Raman beams in free space and in optical fibers has already been studied in [18].

VI. Case of Parasitic Vibrations

As already stated before, the same formalism can be used to evaluate the degradation of the sensitivity to inertial forces caused by parasitic vibrations due to the movement of the retroreflecting mirror.

The sensitivity of the interferometer is then given by

$$\sigma_\Phi^2(\tau) = \frac{k_{\text{eff}}^2}{\tau}\sum_{n=1}^{\infty} |H(2\pi n f_c)|^2\, S_z(2\pi n f_c) \tag{18}$$

where $S_z(\omega)$ is the power spectral density of position noise. Introducing the power spectral density of acceleration noise $S_a(\omega)$, the previous equation can be written as

$$\sigma_\Phi^2(\tau) = \frac{k_{\text{eff}}^2}{\tau} \sum_{n=1}^{\infty} \frac{|H(2\pi n f_c)|^2}{(2\pi n f_c)^4} S_a(2\pi n f_c). \tag{19}$$

It is important to note here that the acceleration noise is severely filtered by the transfer function for acceleration which decreases as $1/f^4$.

In the case of white acceleration noise S_a, and to first order in τ_R/T, the limit on the sensitivity of the interferometer is given by

$$\sigma_\Phi^2(\tau) = \frac{k_{\text{eff}}^2 T^4}{2} \left(\frac{2T_c}{3T} - 1 \right) \frac{S_a}{\tau}. \tag{20}$$

To put this into numbers, we now calculate the requirements on the acceleration noise of the retroreflecting mirror to reach a sensitivity of 1 mrad/shot. For the typical parameters of our gravimeter, the amplitude noise should lie below 10^{-8} m $\cdot$ s^{-2} $\cdot$ Hz$^{-1/2}$. The typical amplitude of the vibration noise measured on the lab floor is 2×10^{-7} m $\cdot$ s^{-2} $\cdot$ Hz$^{-1/2}$ at 1 Hz and rises up to about 5×10^{-5} m $\cdot$ s^{-2} $\cdot$ Hz$^{-1/2}$ at 10 Hz. This vibration noise can be lowered to a few 10^{-7} m $\cdot$ s^{-2} $\cdot$ Hz$^{-1/2}$ in the 1- to 100-Hz frequency band with a passive isolation platform. To fill the gap and cancel the effect of vibrations, one could use the method proposed in [18], which consists of measuring the vibrations of the mirror with a very low noise seismometer and compensating the fluctuations of the position of the mirror by reacting on the Raman laser phase difference.

VII. Conclusion

We have here calculated and experimentally measured the sensitivity function of a three-pulse atomic interferometer. This enables us to determine the influence of the Raman phase noise, as well as of parasitic vibrations, on the noise on the interferometer phase. Reaching a 1 mrad/shot to shot fluctuation requires a very low phase noise frequency reference and an optimized PLL of the Raman lasers, together with a very low level of parasitic vibrations. With our typical experimental parameters, this would result in a sensitivity of 4×10^{-8} rad $\cdot$ s^{-1} $\cdot$ Hz$^{-1/2}$ for the gyroscope and of 1.5×10^{-8} m $\cdot$ s^{-2} $\cdot$ Hz$^{-1/2}$ for the gravimeter. One can then expect that, compared to previous experiments [4], the vibration noise will be, by far, the dominant limitation on the sensitivity of the gravimeter, as reaching the equivalent level of vibration is very difficult.

Improvements on the contribution of some of the noise sources are still possible. The frequency reference could be obtained from an ultrastable microwave oscillator, such as a cryogenic sapphire oscillator [19], whose phase noise lies well below the best quartz available. In addition, the requirements on the phase noise would be easier to achieve using atoms with a lower hyperfine transition frequency, such as Na or K. Trapping a very large initial number of atoms in the 3-D-MOT would enable a very drastic velocity selection. The duration of the Raman pulses could then be significantly increased, which makes the interferometer less sensitive to high-frequency Raman phase noise. The manipulation of the atoms can also be implemented using Bragg pulses [20], [21]. Because difference in the frequencies of the two beams is much smaller, the requirement on the stability of the relative phase is far less stringent. In that case, a different detection method needs to be implemented as atoms in both exit ports of the interferometer are in the same internal state. Using ultracold atoms with subrecoil temperature, atomic wave packets at the two exit ports can be spatially separated, which allows for a simple detection based on absorption imaging. Such an interferometer would benefit from the long interaction times available in space to reach a very high sensitivity.

We also want to emphasize that the sensitivity function can also be used to calculate the phase shifts arising from all possible systematic effects such as the light shifts, magnetic field gradients, and cold atom collisions.

Acknowledgment

The authors would like to thank A. Clairon for fruitful discussions and careful reading of the manuscript.

References

[1] A. Clairon, P. Laurent, G. Santarelli, S. Ghezali, S. N. Lea, and M. Bahoura, "A cesium fountain frequency standard: Preliminary result," *IEEE Trans Instrum. Meas.*, vol. 44, no. 2, pp. 128–131, Apr. 1995.

[2] F. Riehle, T. Kister, A. Witte, J. Helmcke, and C. J. Bordé, "Optical Ramsey spectroscopy in a rotating frame: Sagnac effect in a matter-wave interferometer," *Phys. Rev. Lett.*, vol. 67, no. 2, pp. 177–180, Jul. 1991.

[3] T. L. Gustavson, A. Landragin, and M. Kasevich, "Rotation sensing with a dual atom-interferometer Sagnac gyroscope," *Class. Quantum. Grav.*, vol. 17, no. 12, pp. 2385–2398, 2000.

[4] A. Peters, K. Y. Chung, and S. Chu, "High-precision gravity measurements using atom interferometry," *Metrologia*, vol. 38, no. 1, pp. 25–61, Feb. 2001.

[5] P. R. Berman, Ed., *Atom Interferometry*. Chestnut Hill, MA: Academic, 1997.

[6] T. M. Niebauer, G. S. Sasagawa, J. E. Faller, R. Hilt, and F. Klopping, "A new generation of absolute gravimeters," *Metrologia*, vol. 32, no. 3, pp. 159–180, 1995.

[7] G. E. Stedman, "Ring-laser tests of fundamental physics and geophyscics," *Rep. Prog. Phys.*, vol. 60, pp. 615–688, 1997.

[8] F. Leduc, D. Holleville, J. Fils, A. Clairon, N. Dimarcq, and A. Landragin, "Cold atom gyroscope for precision measurement," in *Proc. ICOLS*, 2003, pp. 68–70.

[9] P. Cheinet, F. Pereira Dos Santos, A. Clairon, N. Dimarcq, D. Holleville, and A. Landragin, "Gravimètre à atomes froids," *J. Phys. 4*, vol. 119, p. 153, 2004.

[10] G. Genevès, P. Gournay, A. Gosset, M. Lecollinet, F. Villar, P. Pinot, P. Juncar, A. Clairon, A. Landragin, D. Holleville, F. Pereira Dos Santos, J. David, M. Besbes, F. Alves, L. Chassagne, and S. Topçu, "The BNM Watt balance project," *IEEE Trans. Instrum. Meas.*, vol. 54, no. 2, pp. 850–853, Apr. 2005.

[11] M. Kasevich and S. Chu, "Atomic interferometry using stimulated Raman transitions," *Phys. Rev. Lett.*, vol. 67, no. 2, pp. 181–184, Jul. 1991.

[12] C. J. Bordé, "Atom interferometry and laser spectroscopy," in *Laser Spectroscopy X*, M. Ducloy, E. Giacobino, and G. Camy, Eds. Singapore: World Scientific, 1991, p. 239.

[13] C. Antoine and C. J. Bordé, "Quantum theory of atomic clocks and gravito-inertial sensors: An update," *J. Opt. B, Quantum Semiclass. Opt.*, vol. 5, no. 2, pp. 199–207, Apr. 2003.

[14] G. J. Dick, "Local oscillator induced instabilities," in *Proc. 19th Annu. Precise Time Time Interval*, 1987, pp. 133–147.

[15] M. Kasevich and S. Chu, "Measurement of the gravitational acceleration of an atom with a light-pulse atom interferometer," *Appl. Phys. B, Laser Opt.*, vol. 54, no. 5, pp. 321–332, May 1992.

[16] K. A. Moler, D. S. Weiss, M. Kasevich, and S. Chu, "Theoretical analysis of velocity-selective Raman transitions," *Phys. Rev. A, Gen. Phys.*, vol. 45, no. 1, pp. 342–348, Jan. 1992.
[17] G. Santarelli, A. Clairon, S. N. Lea, and G. M. Tino, "Heterodyne optical phase locking of extended-cavity semiconductor lasers at 9 GHz," *Opt. Commun.*, vol. 104, no. 4–6, pp. 339–344, Jan. 1994.
[18] F. Yver-Leduc, P. Cheinet, J. Fils, A. Clairon, N. Dimarcq, D. Holleville, P. Bouyer, and A. Landragin, "Reaching the quantum noise limit in a high-sensitivity cold-atom inertial sensor," *J. Opt. B, Quantum Semiclass. Opt.*, vol. 5, no. 2, pp. S136–S142, Apr. 2003.
[19] A. Mann, C. Sheng, and A. Luiten, "Cryogenic sapphire oscillator with exceptionally high frequency stability," *IEEE Trans. Instrum. Meas.*, vol. 50, no. 2, pp. 519–521, Apr. 2001.
[20] E. M. Rasel, M. K. Oberthaler, H. Batelaan, J. Schmiedmayer, and A. Zeilinger, "Atom wave interferometry with diffraction gratings of light," *Phys. Rev. Lett.*, vol. 75, no. 14, pp. 2633–2637, Oct. 1995.
[21] D. M. Giltner, R. W. McGowan, and S. A. Lee, "Atom interferometer based on Bragg scattering from standing light waves," *Phys. Rev. Lett.*, vol. 75, no. 14, pp. 2638–2641, Oct. 1995.

Patrick Cheinet received the Ph.D. degree in physics from the Université Paris VI, Paris, France, in 2006.

He is currently a Postdoctoral Fellow with the University of Mainz, Mainz, Germany. His research interests include Bose Einstein condensates, ultracold gases in optical lattices, and strongly correlated many body physics.

Benjamin Canuel received the degree in physics and the Ph.D. degree in physics from the Université Paris XI, Orsay, France, in 2003 and 2007.

He is currently an Applied Physicist with the European Gravitational Observatory, Pisa, Italy. His research interests include optical systems for gravitational wave detection, high-power stabilized lasers, and nonlinear optics.

Franck Pereira Dos Santos was born in Fontainebleau, France, on April 30, 1973. He received the degree from Ecole Normale Supérieure, Paris, France, and the Ph.D. degree in physics from the Université Pierre et Marie Curie, Paris VI, in 2002.

Since 2002, he has been with the Laboratoire National de Métrologie et d'Essais-Systèmes de Référence Temps Espace (LNE-SYRTE), Observatoire de Paris, Paris, France, where he currently works on the development of cold atomic sensors. Since October 2004, he has been a permanent Researcher with CNRS. His research interests include laser cooling and Bose Einstein condensation.

Alexandre Gauguet received the degree from the University of Orsay, Orsay, France, in 2004. He is currently working toward the Ph.D. degree with the Laboratoire National de Métrologie et d'Essais-Systèmes de Référence Temps Espace, (LNE-SYRTE), Observatoire de Paris, Paris, France.

Florence Yver-Leduc graduated from the Institut d'Optique, Orsay, France, in 2001 and received the Ph.D. degree in physics from the Université Paris XI, Orsay, in 2004.

He is currently with the Laboratoire National de Métrologie et d'Essais-Systèmes de Référence Temps Espace, (LNE-SYRTE), Observatoire de Paris, Paris, France.

Arnaud Landragin received the Ph.D. degree in physics from the Université Paris XI, Orsay, France, in 1997.

He is currently a permanent Researcher with the Laboratoire National de Métrologie et d'Essais-Systèmes de Référence Temps Espace, (LNE-SYRTE), Observatoire de Paris, Paris, France. His research interests include the realization and characterization of atom interferometers for application as inertial sensors.